Pyrolysis of Golden Snail Shells (*Pomacea canaliculata* L.) for Phosphorus Removal from Aqueous Solutions

M. T. Vu,[a] L.-T.-T.-T. Hoang,[b,c] and M.-T. Dao[d,*]

[a]Hanoi University of Natural Resources and Environment, Ministry of Natural Resources and Environment, 41 Phu Dien, Bac Tu Liem, Ha Noi, 100000, Vietnam

[b]Laboratory of Advanced Materials Chemistry, Institute for Advanced Study in Technology, Ton Duc Thang University, Ho Chi Minh City, Vietnam

[c]Faculty of Applied Sciences, Ton Duc Thang University, Ho Chi Minh City, Vietnam

[d]Department of Environmental Engineering, Thu Dau Mot University, Binh Duong, 820000, Vietnam

doi: https://doi.org/10.15255/CABEQ.2024.2323

Original scientific paper
Received: April 20, 2024
Accepted: November 21, 2024

Biochar derived from abundant waste biomass has emerged as an eco-friendly alternative to conventional adsorbents. In this study, biochar produced from golden snail shells through a simple pyrolysis process was applied for phosphorus adsorption. The effects of pyrolysis temperature and time on adsorption capacity were investigated. The biochar pyrolyzed at 800 °C for 90 min (B800) exhibited the best adsorption performance. Optimal adsorption conditions were determined to be a pH of 4.0 and an adsorbent dose of 1.6 g L^{-1}. The adsorption of phosphorus onto B800 could be well described by the Langmuir model and the pseudo-first-order model, achieving a maximum adsorption capacity of 63.5 mg g^{-1} and a rate constant of 0.029 min^{-1}. This study highlights the potential of biochar derived from agricultural waste as a highly efficient and environmentally friendly adsorbent for phosphorus removal. Furthermore, the adsorption mechanism, driven by the electrostatic interaction occurring prior to Ca-P precipitation, was elucidated. The phosphorus adsorbed onto biochar can potentially be recycled as a soil fertilizer.

Keywords
biochar, golden snail, phosphorus removal, pyrolysis

Introduction

The rapid expansion of urbanization, industrialization, and agricultural activities generates significant quantities of wastewater polluted with heavy metals, dyes, toxic anions, and organic matter. Among these pollutants, untreated phosphorus from sources such as agriculture[1,2], industries[1,3], soil management[2], and the use of fertilizers, pesticides, and phosphorus-containing detergents[2,3], poses multiple challenges. Phosphorus-laden water sources are particularly susceptible to eutrophication, which involves a process characterized by excessive growth of algae[4]. This uncontrollable algal proliferation reduces water transparency, inhibiting photosynthesis[4,5]. Additionally, algal decomposition drastically depletes dissolved oxygen, releasing harmful toxins and gases, as well as foul odors[4,5], thereby threatening aquatic ecosystems and degrading water quality[4,5]. Over time, these conditions render water unsuitable for consumption. Many reports have linked various human health issues, such as impaired mineral metabolism, chronic kidney disease, cardiovascular complications, and bone loss[7–9], with the consumption of water from these polluted sources[6].

Given these adverse effects, pre-treatment of phosphorus-laden wastewater is a crucial step to ensure safe discharge levels[2]. Many techniques have been developed and applied with various advantages and disadvantages. These techniques include chemical precipitation[3,10], electrocoagulation[11], ion exchange, membrane separation[3,12], and biological removal[12,13]. Notably, adsorption has garnered significant attention for its high efficiency and ease of regeneration[3,12,14]. A variety of adsorbents, such as chemically modified clay, zeolites, synthetic materials containing metal oxides or hydroxides[14], and natural minerals[12], have been developed. However, the high cost of synthesis, strong dependence on environmental conditions, and large dosage require-

*Corresponding author: Email: trungdm@tdmu.edu.vn

ments have limited their performance in practical treatment[12]. In this context, biochar derived from eco-friendly, abundant waste biomasses has emerged as a promising alternative to conventional adsorbents[12,14]. Among the various biochar production methods, pyrolysis stands out due to its rapid process, feasibility for large-scale production, high recovery of products that are advantageous for adsorptive action[15] and thermally stable[16].

The excellent adsorption performance of biochar is demonstrated through its unique properties, including a porous carbon network, large surface area, and diverse functional groups[12]. Moreover, after phosphorus adsorption, the biochar can be re-purposed as a phosphorus-rich fertilizer, which can be directly applied to the soil without desorption[17]. This approach can improve soil structure, improve its water and moisture holding capacity, and provide microbial biomass[18–22]. This distinctive feature has advanced biochar as a sustainable material for phosphorus removal.

To enhance the adsorption affinity of biochar for phosphorus, pure biochar has been modified using metal cations in ionic or oxide forms[23]. Compared to unmodified biochar, modified biochar demonstrates superior phosphorus adsorption capacity stimulated by electrostatic or chemical interaction between metallic components and phosphorus within aqueous solutions[12,24–26]. Among various metal cations, Ca^{2+} ions are widely favored for biochar modification due to their high availability, low cost, and non-toxic nature[27]. Biochar modified with calcium derived from agricultural wastes such as orange peel[28], corn stover[29], or yellow pine[30], has shown significant phosphate uptake at 23.2, 33.9, and 138.7 mg g^{-1}, respectively. This was mainly attributed to the Ca–O and Ca–OH sites present on the adsorbent surfaces at basic pH, promoting phosphate adsorption and ligand exchange, or Ca^{2+} leaches from the surface at acidic pH, precipitating phosphates[27]. However, due to using large quantities of chemicals, modification processes can be time-consuming, expensive, and potentially harmful to the environment[23]. Consequently, there is growing interest in developing biochar from natural materials having high levels of metal ions through a single-step pyrolysis process using waste biomass.

Golden snail (*Pomacea canaliculata* L.) shells consist of a prismatic layer rich in calcium, primarily in the form of calcium carbonate, making them a promising material for Ca-biochar preparation[31]. This species of snail is notorious as one of the most harmful pests, causing significant damage to crops, especially aquatic crops such as rice[31–34]. In wastewater treatment, this bio-waste has been found to have high potential for removing Pb(II), Cd(II), and Cu(II) ions[35], as well as for reducing Biochemical Oxygen Demand (BOD) and Chemical Oxygen Demand (COD)[36]. Utilizing golden snail shell for this approach can encourage farmers to collect these pests, reducing their proliferation and associated crop damage, while providing additional income[35]. To the best of our knowledge, the application of biochar derived from golden snail shell for phosphorus removal has not yet been reported. In this study, biochar was prepared from golden snail shell, an abundant bio-waste in Vietnam, through a single-step pyrolysis process. The material's properties, including surface morphology and functional groups, were characterized under varying pyrolysis conditions. The phosphorus removal performance of the obtained biochar was also evaluated.

Materials and methods

Chemicals and materials

Anhydrous potassium dihydrogen phosphate (KH_2PO_4), ascorbic acid, hexammonium heptamolybdate 4-hydrate ($(NH_4)_6MO_7O_{24}{\cdot}4H_2O$), potassium antimony tartrate ($K(SbO)C_4H_4O_6{\cdot}0.5H_2O$), sulfuric acid ($H_2SO_4$), hydrochloric acid (HCl), and sodium hydroxide (NaOH) of analytical grade were used as received. The golden snails (*P. canaliculata* L.) were collected from the fields located at Lien Hoa Commune, Dong Hung District, Thai Binh Province, Vietnam.

Preparation of biochar from golden snail shell

The collected golden snail shells were thoroughly washed and dried at ambient conditions. The shells were then ground and sieved to yield a raw powder (R0) with a particle size of 1–2 mm. The pyrolyzed biochars were prepared using a muffle furnace (Nabertherm L3/11/B170, Germany) in the absence of oxygen. The pyrolysis process was performed by programming the furnace controller to consecutively raise the internal temperature of the biomass chamber to 300, 400, 500, 600, 700, and 800 °C, at a rate of 5 °C min^{-1}, and maintained for 2 h. These biochars were respectively denoted as B300, B400, B500, B600, B700, and B800. The process was then conducted by holding the peak temperature at 800 °C for different intervals, including 30, 60, 90, 120, and 180 min. The cooled-to-ambient-temperature materials were allowed to disintegrate into smooth and fine powder, which was sealed in a container before use. To evaluate the effect of pyrolysis temperature and time on the performance of the prepared biochars, their phosphorus adsorption capacities were investigated.

Material characterizations

The surface morphology and energy-dispersive X-ray (EDX) spectrum of the materials were examined using scanning electron microscopy (SEM, Hitachi S4800 NIHE) equipped with an EDX system. The system was operated at an accelerating electron voltage of 10.0 kV and a magnification of x25k and x10k. The NEXUS 670, Nicole FT–IR spectrophotometer was used to obtain the transmission infrared spectra of samples/KBr pellets. In detail, each sample was thoroughly mixed with KBr (FT–IR grade) and pressed to prepare a pellet, which was then applied to the sample holder for FT–IR recording. To identify the crystalline phases, X-ray diffraction (XRD) was applied using a D8 Advance, Bruker diffractometer equipped with a Cu Kα radiation source at a wavelength of 0.154 nm and a monochromator. The XRD patterns were recorded by scanning 2θ from 10 to 70° with a scanning step width of 0.05° per scan.

Adsorption experiment

The adsorption of phosphorus by the as-synthesized biochars was conducted using batch experiments. In each experiment, 0.4 g of the biochar was added to 250 mL of a solution prepared from anhydrous potassium dihydrogen phosphate (KH_2PO_4). The mixture was shaken continuously. The sample solutions were then collected by filtration. For the study of pyrolysis temperature and pyrolysis time, the solution pH was not adjusted (neutral pH) with the adsorbent dose of 1.6 g L^{-1}, the initial phosphorus concentration of 50 mg L^{-1} and adsorption time of 2 h. To study the effect of solution pH on phosphorus removal efficiency, the initial pH was screened using the HACH HQ440D portable pH meter, and adjusted by 0.1 M HCl and 0.1 M NaOH to different values in the range of 4.0–10.0. The adsorbent dose and phosphorus initial concentration were maintained at 1.6 g L^{-1} and 50 mg L^{-1}, respectively. The influence of the adsorbent dose was investigated in the range of 0.4 to 2.0 g L^{-1} under the initial pH of 4.0, adsorption time of 2 h, and initial phosphorus concentration of 50 mg L^{-1}. The experiments of adsorption kinetics and adsorption isotherms were conducted at sorption time in a range of 60–240 min and 50–1000 mg L^{-1}, respectively. The given data was analyzed by fitting non-linear pseudo-first-order model (Eq. 1), pseudo-second-order model (Eq. 2), and Elovich model (Eq. 3).

$$q_t = q_e(1 - \exp(-k_1 t)) \quad (1)$$

$$q_t = \frac{q_e^2 k_2 t}{q_e k_2 t + 1} \quad (2)$$

$$q_t = \frac{1}{\beta} \ln(1 + \alpha\beta t) \quad (3)$$

where q_t (mg g^{-1}) and q_e (mg g^{-1}) are adsorption capacities at time t and at equilibrium, respectively. k_1 (min^{-1}) and k_2 (g mg^{-1} min^{-1}), α (mg g^{-1} min^{-1}) are respectively the rate constant of the pseudo-first-order, pseudo-second-order kinetics, and Elovich models. β (mg g^{-1}) is the desorption constant in the Elovich equation. Regarding sorption isotherms, investigation under various phosphorus initial concentrations of 50, 100, 150, 200, 400, 600, 800, 1000 mg L^{-1} were performed.

The initial and equilibrium concentrations of phosphorus ion were measured by the colorimetric method using molybdenum blue color reagent for phosphorus detection. This reagent was prepared using hexammonium heptamolybdate 4-hydrate ($(NH_4)_6MO_7O_{24}\cdot 4H_2O$), potassium antimony tartrate ($K(SbO)C_4H_4O_6\cdot 0.5H_2O$), ascorbic acid, sulfuric acid, and hydrochloric acid, following the procedure of Angelova *et al*.[37] The identification of phosphorus concentration was performed by an ultraviolet-visible (UV-VIS) spectrometer (Hach, DR5000, USA) at a wavelength of 880 nm[37]. The adsorption capacity of the adsorbents was calculated using Eq. (4):

$$q_e = \frac{(c_0 - c_t)\cdot V}{m} \quad (4)$$

where c_0 and c_t are the initial concentration and the concentration of PO_4^{3-} anion at a given time t (mg L^{-1}), respectively; m is the weight of the adsorbent (g), and V is the treated solution volume (V).

Results and discussion

Biochar characterization

XRD

The XRD patterns of R0, B700 and B800 are shown in Fig. 1a. The R0 is composed of a poorly crystalline aragonite phase, a common phase of $CaCO_3$ (PDF no. 00-041-1475). This observation aligns with previous studies on this type of shell[35,38]. Upon pyrolysis of the snail shell at high temperature, the aragonite phase transitioned into the calcite phase (PDF no. 01-086-4273) as evident in the XRD patterns of B700 and B800. The sharp and intense peaks observed for these calcined samples confirmed the crystalline nature of the biochars.

FT-IR

FT–IR spectra of R0, B700 and B800, recorded in the range of 4000 to 400 cm^{-1} (Fig. 1b), exhibited characteristic vibration peaks corresponding to CO_3^{2-} ions. The prominent absorption peak at 1446 cm^{-1} can be assigned to asymmetric stretching[39]. The other two absorption bands at 859 and 711 cm^{-1}

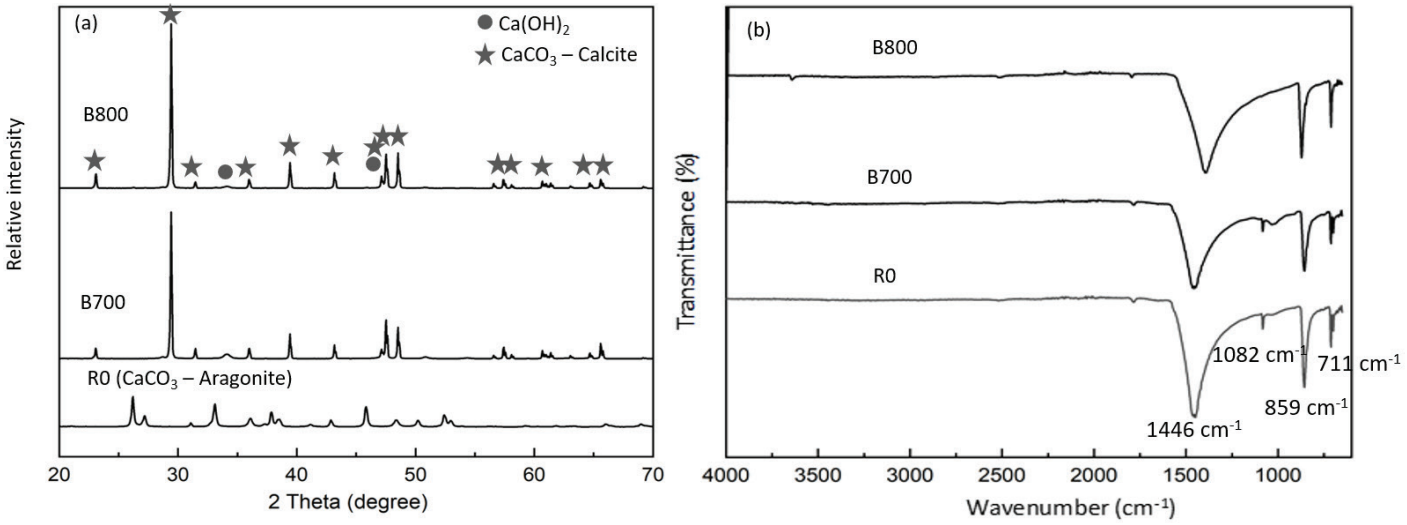

Fig. 1 – *XRD patterns (a) and FT-IR spectra (b) of R0, B700 and B800*

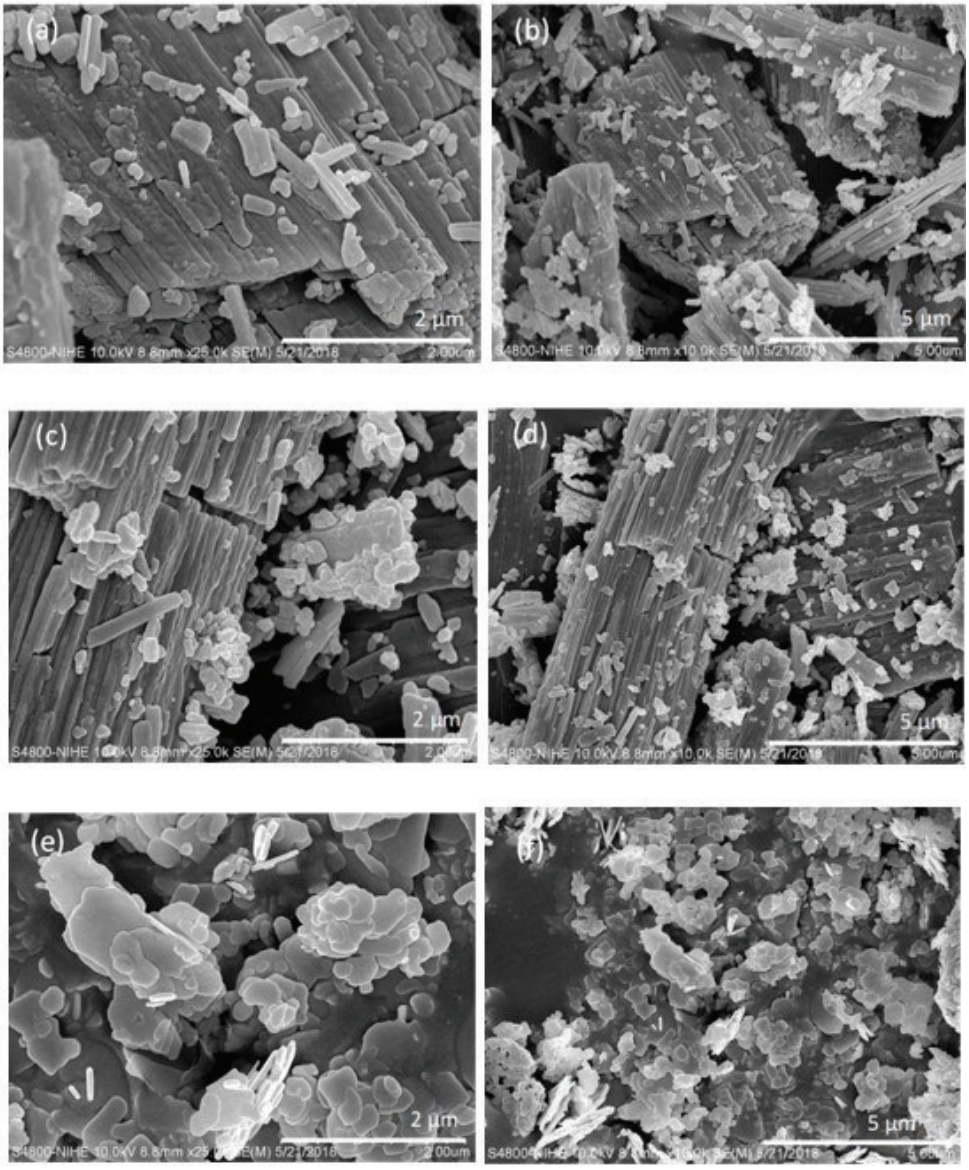

Fig. 2 – *SEM images of R0 (a–b), B700 (c–d), and B800 (e–f)*

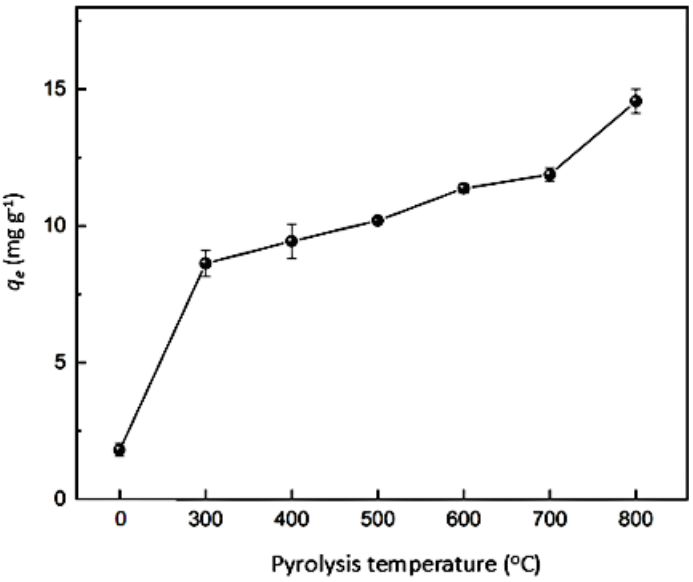

Fig. 3 – *Effect of pyrolysis temperature on phosphorus adsorption capacity (pH: neutral; Biochar dose: 1.6 g L^{-1}; Phosphorus initial concentration: 50 mg L^{-1}; Adsorption time: 2 h; Temperature: RT)*

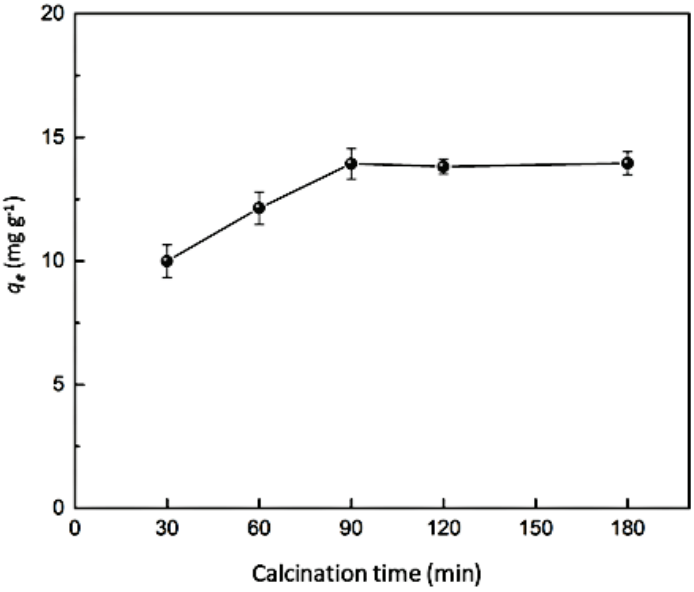

Fig. 4 - *Effect of pyrolysis time on phosphorus adsorption capacity (pH: neutral; Biochar dose: 1.6 g L^{-1}; Phosphorus initial concentration: 50 mg L^{-1}; Adsorption time: 2 h; Temperature: RT)*

could be attributed to out-of-plane band and in-plane band modes of vibration for the CO_3^{2-} molecules, respectively[39]. A weak absorption band at 1082 cm^{-1}, observed in R0 and B700,[40,41] corresponded to symmetric stretching of CO_3^{2-} molecules.

SEM

The surface morphology of the R0, B700, and B800 samples was examined, and is presented in Fig. 2. The R0 and B700 consisted of large adhesive particles which were regular and cylindrical. For B800, the morphology was distinctive with plate-like shapes with smaller particles.

Phosphorus removal

Effect of pyrolysis temperature

The alteration of phosphorus removal capacity at varied pyrolysis temperatures is presented in Fig. 3. As evident, the adsorption capacities of all biochars were higher than that of the raw shell. As the pyrolysis temperature increased from 300 to 800 °C, the adsorption capacity of the biochars improved from 8.63 to 14.56 mg g^{-1}. This trend is consistent with prior studies highlighting the significant influence of pyrolysis temperature on phosphorus uptake[42,43]. The pyrolysis temperature of 800 °C was therefore selected for subsequent investigations.

Effect of pyrolysis time

The influence of pyrolysis time on phosphorus removal is depicted in Fig. 4. The adsorption capacity gradually increased with prolonged pyrolysis time, reaching a maximum of 13.94 mg g^{-1} at 90 min. Extending the pyrolysis time to 180 min. did not result in a statistically significant improvement in the biochars' adsorption capacity at a 95 % confidence interval (α = 0.05, one-way ANOVA, P = 0.94). These data are consistent with the findings of Adhikari *et al.*[42] and Ramola *et al.*[43] Therefore, a pyrolysis time of 90 minutes was deemed reasonable.

Effect of pH

The removal of phosphorus species by adsorption strongly depends on the pH of the aqueous media, as it may cause modifications in the surface net charge of the biochar in addition to phosphorus speciation[41]. In this study, the obtained data on the effect of initial pH (Fig. 5a) indicated that the adsorption capacity of the biochar decreased as the pH increased from 4.0 to 10.0. This finding was in agreement with the studies by Gold *et al.*[44] and Adaramaja *et al.*[45], reporting similar biochars prepared from calcined snail shell (800 °C, 2 h) with pH_{pzc} at 11.0. This suggests that the biochar surface exhibits a positive charge across a wide pH range, resulting in strong electrostatic affinity for negatively charged phosphorus ions[45]. Accordingly, in this study, at pH < 11.0, the biochar possibly carried a positive charge, enabling attraction of negatively charged phosphorus ions in the solution, thus promoting the adsorption process. It is worth noting that, when the pH rose from 4.0 to 11.0, the material's surface became less positively charged, weakening the electrostatic attraction with phosphorus species, and reducing adsorption capacity[46].

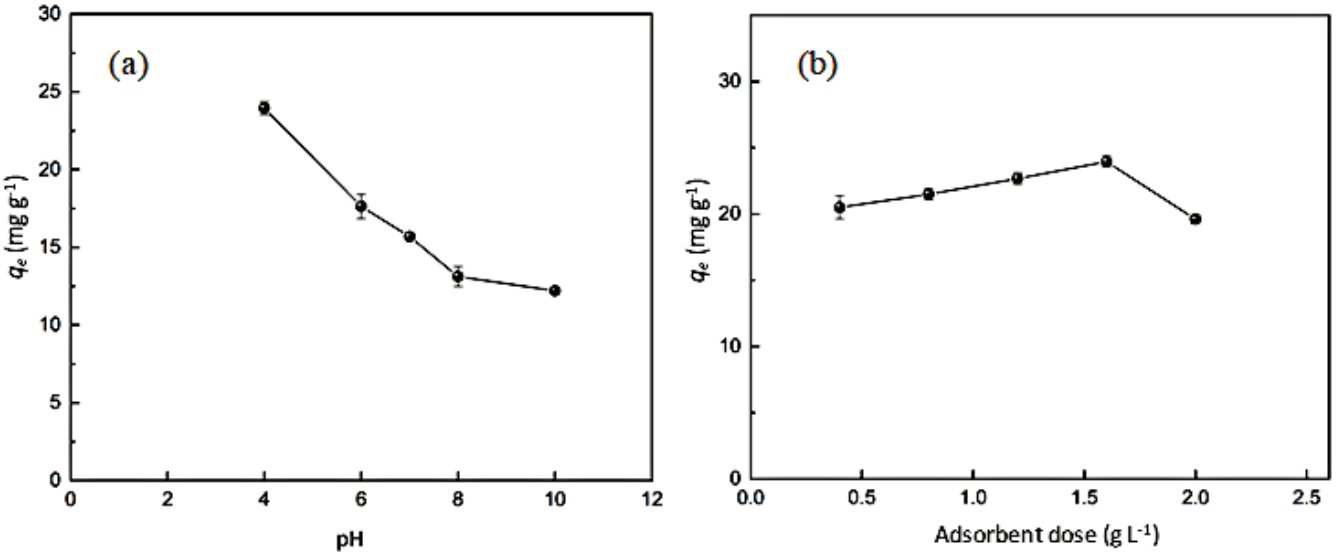

Fig. 5 – *(a) Effect of initial pH on phosphorus adsorption capacity (Biochar dose: 1.6 g L^{-1}; Phosphorus initial concentration: 50 mg L^{-1}; Adsorption time: 2 h; Temperature: RT); (b) Effect of adsorbent dose on phosphorus adsorption capacity (pH: 4.0; Phosphorus initial concentration: 50 mg L^{-1}; Adsorption time: 2 h; Temperature: RT)*

Effect of adsorbent dose

The effect of adsorbent dose on the adsorption performance of B800 was evaluated at varying adsorbent doses of 0.4, 0.8, 1.2, 1.6, and 2.0 g L^{-1} (Fig. 5). Increasing the dose from 0.4 to 1.6 g L^{-1}, steadily enhanced the removal capacity, reaching the highest value of 23.95 mg g^{-1}. This enhancement was reasonable, as more adsorption sites on the adsorbent were introduced to interact with phosphorus species. Beyond this threshold, the removal capacity decreased to 19.60 mg g^{-1} at a dose of 2.0 g L^{-1}. This sudden decline may be attributed to the agglomeration of biochar at higher dosages, which drastically blocked available adsorption sites[47].

Adsorption kinetics

The adsorption of phosphorus by B800 was conducted at different contact times (Fig. 6). The process occurred rapidly within the first hour, and reached equilibrium after 2 h. The experimental kinetics data were fitted to three models: non-linear pseudo-first-order, pseudo-second-order, and Elovich, to determine the rate of adsorption[48–50]. The parameters derived from these models are summarized in Table 1. The experimental data were well described by the pseudo-first-order model. The similarity of equilibrium adsorption capacity (q_e) calculated from the pseudo-first-order model (17.68 mg g^{-1}), and the experimental value (17.70 mg g^{-1}) also supported this statement. The rate constant (k_1) of the pseudo-first-order model was determined to be 0.029 (min^{-1}).

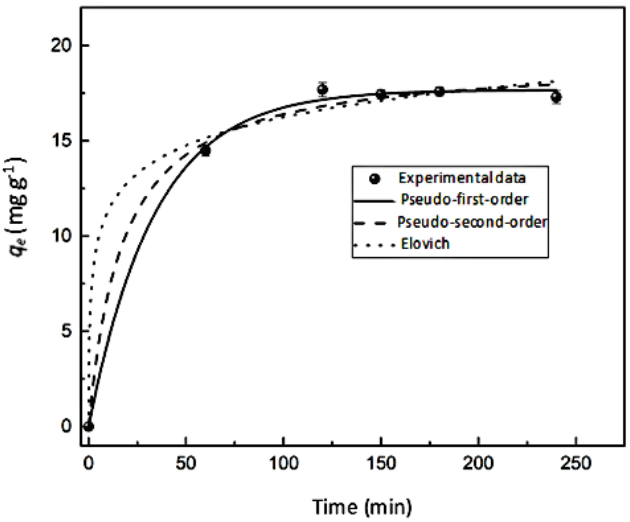

Fig. 6 – *Phosphorus adsorption kinetics of B800 (pH: 6.0; Biochar dose: 1.6 g L^{-1}; Phosphorus initial concentration: 50 mg L^{-1}; Temperature: RT)*

Table 1 – *Kinetics model parameters in the adsorption of phosphorus performed by B800*

Kinetic models and corresponding equations	Kinetic model parameters and regression coefficients		
Pseudo-first-order	k_1 (min^{-1})	q_e (mg g^{-1})	R^2
	0.029	17.68	0.998
Pseudo-second-order	k_2 (g mg^{-1} min^{-1})	q_e (mg g^{-1})	R^2
	0.0029	19.29	0.994
Elovich	α (mg g^{-1} min^{-1})	β (mg g^{-1})	R^2
	42.21	0.47	0.990

Adsorption isotherms

The adsorption isotherm experiments were conducted to investigate the adsorption behavior at equilibrium. The effect of phosphorus concentration on the adsorption capacity of B800 is presented in Fig. 7. The phosphorus adsorption capacity increased with the increase in phosphorus initial concentration. The obtained data were further analyzed using non-linear Langmuir, Freundlich, and Temkin isotherm models, with their respective equations provided in Table 2 and non-linear plots shown in Fig. 7. It can be observed that the isotherm data expressed a better fit with the Langmuir model (R^2 = 0.966) compared to the Freundlich (R^2 = 0.902) and Temkin models (R^2 = 0.948). The maximum adsorption capacity of B800 obtained from the Langmuir model was 63.5 mg g^{-1}.

The adsorption nature was further examined using the dimensionless constant or separation factor R_L. This value was calculated using Eq. (5) where c_0 and K_L are the initial concentrations of PO_4^{3-} anion and the Langmuir constant, respectively[51]. This value is the essential characteristic of Langmuir isotherm, which allows qualitative assessment of different types of adsorption process, including irreversible if R_L = 0 (very strong adsorption), favorable if 0 < R_L < 1 (normal adsorption), linear if R_L = 1, or unfavorable if R_L > 1 (or desorption)[51]. In the range of initial phosphorus concentrations in this study, the calculated R_L values (Table 2) were all greater than zero but less than one, indicating that a normal equilibrium sorption of phosphorus on the surface of B800 occurred under the experimental conditions. These findings were similar to our previous reports on the potential of biosorbents prepared from *Annona glabra* seeds[52] and *Hylocereus undatus* (dragon fruit) peel[53] for methylene blue and tetracycline removal, respectively.

The maximum adsorption capacity of B800 was determined from the Langmuir model, and compared with previously studied biochars (Table 3). The results revealed that the B800 prepared in this study exhibited a comparable maximum adsorption capacity with other materials, suggesting that this new biosorbent is efficient and suitable for the removal of phosphorus in aqueous media.

$$R_L = \frac{1}{\left(1 + K_L c_0\right)} \tag{5}$$

Adsorption mechanism

The good fit of adsorption isotherms to the Langmuir model suggested monolayer coverage of phosphorus species on the adsorbent surface[25,41,54]. In other words, the reaction of the sorbent and sorbate occurred at the active sites on the material's surface. The interactions between phosphorus spe-

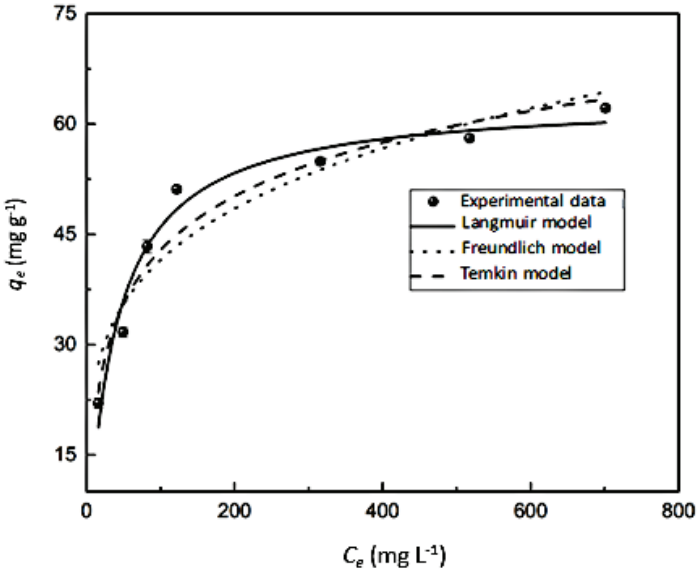

Fig. 7 – *Non-linear adsorption isotherms in the adsorption of phosphorus performed by B800 (pH 4.0; Biochar dose 1.6 g L^{-1}; Adsorption time: 2 h; Temperature: RT)*

Table 2 – *Isotherm parameters in the adsorption of phosphorus performed by B800*

Model and corresponding equation	Adsorption isotherm model parameters	
Langmuir $q_e = \frac{q_m K_L c_e}{1 + K_L c_e}$	q_m (mg g^{-1})	63.5
	K_L (L mg^{-1})	0.026
	R^2	0.966
	R_L	
	50 mg L^{-1}	0.43
	100 mg L^{-1}	0.28
	150 mg L^{-1}	0.20
	200 mg L^{-1}	0.16
	400 mg L^{-1}	0.087
	600 mg L^{-1}	0.059
	800 mg L^{-1}	0.046
	1000 mg L^{-1}	0.037
Freundlich $q_e = K_F c_e^{1/n}$	K_F (mg g^{-1}) (L mg^{-1})$^{1/n}$	14.7
	n	4.4
	R^2	0.903
Temkin $q_e = \frac{RT}{b_T} \ln(A_T c_e)$	b_T (kJ mol^{-1})	0.24
	A_T (L mg^{-1})	0.58
	R^2	0.948

q_e: adsorption capacity at equilibrium of adsorbent; q_m: maximum adsorption capacity;

K_L: Langmuir constant; K_F: Freundlich constant; c_e: equilibrium adsorbate concentration;

b_T: Temkin constant; A_T: Temkin isotherm constant

Table 3 – *Comparison of maximum adsorption capacity (q_m) results of this study with other studies for phosphorus removal*

Adsorbents	q_m (mg g^{-1})
Paper mill sludge biochar[21]	25.19
Hydrochar composites of lanthanum from rice straw[22]	61.57
Ca-impregnated biochar from ramie stem[23]	105.41
Ca-modified biochar prepared from eggshell and sewage sludge via co-pyrolysis[34]	121.01
Mn/Al double oxygen sludge-derived biochar from dewatered sewage sludge[35]	28.20
Mg−biochar nanocomposite from Mg-enriched tomato leaves[41]	103.80
Graphene[42]	89.37
Pine sawdust char[43]	15.11
Zirconic chitosan beads[44]	61.70
Golden snail shell biochar (this study)	63.5

cies and calcium-based materials involves mechanisms such as surface precipitation, surface complexation, dissolution-precipitation, and/or electrostatic interaction[25,41]. It is known that solution pH plays a significant role in these mechanisms of phosphorus adsorption[55], and it might affect each mechanism differently. In the electrostatic interaction, the adsorption capacity may have been promoted at low pH due to the favorable electrostatic attraction between the positively charged adsorbent and the negatively charged phosphorus ions. On the other hand, at higher pH, the number of positively charged sites decreased. Therefore, the electrostatically repulsive force between the adsorbent and the negatively charged phosphorus ions became more favorable, decreasing the adsorption capacity. For the precipitation mechanism, the low pH might have induced the formation of dicalcium phosphate and octacalcium phosphate, while higher pH tended to lead to calcium-deficient hydroxyapatite and hydroxyapatite[56].

To elucidate the adsorption mechanism, the used adsorbent was analyzed using XRD, SEM, and EDX techniques (Fig. 8). The intensity associated with P in the EDX spectrum was identified, confirming the removal of phosphorus from the aqueous solutions and its existence in the used adsorbent. The XRD analysis revealed that these phosphorus ions existed in brushite phase $CaHPO_4{\cdot}2H_2O$ (PDF no. 01-072-1240) alongside the calcite phase of $CaCO_3$ in the material. The formation of brushite is consistent with the results regarding the effect of pH on adsorption capacity that the adsorption process was favorable at low pH. This indicates the mechanism of the process based on the electrostatic interaction occurring prior to precipitation. At low pH, the positively charged biochar electrostatically attracts negatively charged phosphorus ions species, favoring the precipitation of dicalcium phosphate. In contrast, at higher pH, electrostatic repulsion was observed between the two negatively charged, inhibiting the interaction and precipitation of calcium and phosphorus ions.

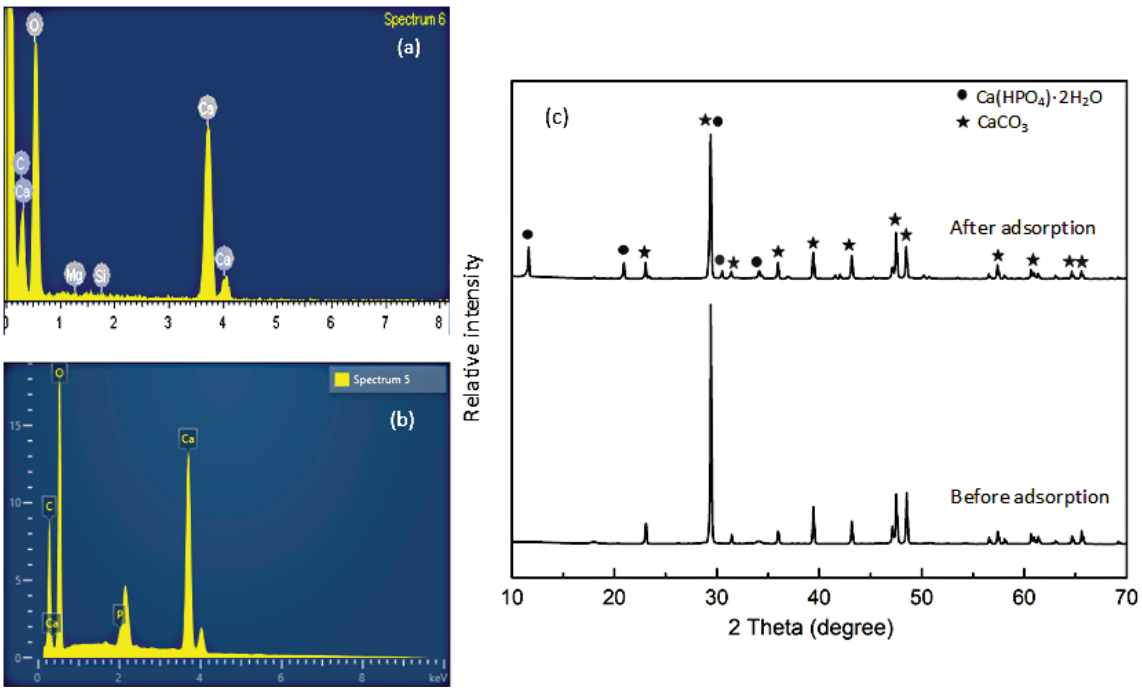

Fig. 8 – *B800: EDX spectrum (a) before and (b) after the adsorption. XRD spectrum (c) before and after the adsorption.*

Conclusions

In this study, biochar was synthesized from golden snail shell biomass waste using single-step pyrolysis, optimized at 800 °C for 90 min. The finest biochar had small, plate-like particles. Phosphorus removal experiments revealed the strong dependence of biochar's adsorption capacity on the initial pH and the adsorbent dose. Adsorption kinetics and isotherms of the investigated adsorbent/adsorbate system were best fitted with the pseudo-first-order and the Langmuir models. Electrostatic interactions and precipitation between phosphorus species and the calcium-based biochar were identified as the major mechanisms, which were most favorable at low pH. The as-synthesized biochar exhibited great potential for phosphorus removal, offering high performance and cost-effectiveness. Furthermore, its preparation from golden snail shell bio-waste makes this material a promising and eco-friendly solution for wastewater treatment and waste disposal.

DATA AVAILABILITY STATEMENT

The data used to support the findings of this study are included within the article.

DISCLOSURE OF CONFLICT OF INTEREST

The authors report there are no competing interests to declare.

FUNDING STATEMENT

The authors declare that no funds, grants, or other support were received during the preparation of this manuscript.

References

1. *Carpenter, S. R., Caraco, N. F., Correll, D. L., Howarth, R. W., Sharpley, A. N., Smith, V. H.,* Nonpoint pollution of surface waters with phosphorus and nitrogen, Ecol. Appl. **8**(3) (1998) 559. doi: https://doi.org/10.1890/1051-0761(1998)008[0559:NPOSWW]2.0.CO;2
2. *Mutenita, C., Balanica, C. M. D., Simionescu, A. G., Stanciu, S., Popa, C. L.,* The efficiency of biological total phosphorus removal process, Rev. Chim. (Bucharest) **70**(3) (2019) 1920. doi: https://doi.org/10.37358/RC.19.6.7247
3. *Li, Y., Nan, X., Li, D., Wang, L., Xu, R., Li, Q.,* Advances in the treatment of phosphorus-containing wastewater, IOP Conf. Ser.: Earth Environ. Sci. **647** (2021). doi: https://doi.org/10.1088/1755-1315/647/1/012163
4. *Bennett, E. M., Carpenter, S. R., Caraco, N. F.,* Human impact on erodible phosphorus and eutrophication: A global perspective, Bioscience **51**(3) (2001) 227. doi: https://doi.org/10.1641/0006-3568(2001)051[0227:HIOEPA]2.0.CO;2
5. *Yang, X., Wu, X., Hao, H., He, Z.,* Mechanisms and assessment of water eutrophication, J. Zhejiang Univ. Sci. B. **9**(3) (2008) 197. doi: https://doi.org/10.1631/jzus.B0710626
6. *Calvo, M. S., Uribarri†, J.,* Contributions to total phosphorus intake: All sources considered, Seminars in Dialysis **26**(1) (2012a) 54. doi: https://doi.org/10.1111/sdi.12042
7. *Calvo, M. S., Kumar, R., III Heath, H.,* Persistently elevated parathyroid hormone secretion and action in young women after four weeks of ingesting high phosphorus, low calcium diets, J. Clin. Endocrinol. Metab. **70** (1990) 1334. doi: https://doi.org/10.1210/jcem-70-5-1334
8. *Calvo, M. S., Uribarri†, J.,* Public health impact of dietary phosphorus excess on bone and cardiovascular health in the general population, Am. J. Clin. Nutr. **98**(1) (2012b) 6. doi: https://doi.org/10.3945/ajcn.112.053934
9. *Cancela, A. L., Santos, R. D., Titan, S. M., Goldenstein, P. T., Rochitte, C. E., Lemos, P. A., Reis dos, L. M., Graciolli, F. G., Jorgetti, V., Moysés, R. M.,* Phosphorus is associated with coronary artery disease in patients with preserved renal function, PLOSone **7**(5) (2012) e36883. doi: https://doi.org/10.1371/journal.pone.0036883
10. *Yu, Y., Wu, R., Clark, M.,* Phosphate removal by hydrothermally modified fumed silica and pulverized oyster shell, J. Colloid Interface Sci. **350** (2010) 538. doi: https://doi.org/10.1016/j.jcis.2010.06.033
11. *Zangarini, S., Sciarria, T. P., Tambone, F., Adani, F.,* Phosphorus removal from livestock effluents: Recent technologies and new perspectives on low-cost strategies, Environ. Sci. Pollut. Res. **27** (2020) 5730. doi: https://doi.org/10.1007/s11356-019-07542-4
12. *Zahed, M. A., Salehi, S., Tabari, Y., Farraji, H., Ataei-Kachooei, S., Zinatizadeh, A. A., Kamali, N., Mahjouri, M.,* Phosphorus removal and recovery: State of the science and challenges, Environ. Sci. Pollut. Res. **29** (2022) 58561. doi: https://doi.org/10.1007/s11356-022-21637-5
13. *Liu, R., Hao, X., Chen, Q., Li, J.,* Research advances of Tetrasphaera in enhanced biological phosphorus removal: A review, Water Research **166** (2019). doi: https://doi.org/10.1016/j.watres.2019.115003
14. *Ramasahayam, S. K., Guzman, L., Gunawan, G., Viswanathan, T.,* A comprehensive review of phosphorus removal technologies and processes, J. Macromol. Sci. Part A: Pure. Appl. Chem. **51** (2014) 538. doi: https://doi.org/10.1080/10601325.2014.906271
15. *Gabhane, J. W., Bhange, V. P., Patil, P. D., Kumar, S.,* Recent trends in biochar production methods and its application as a soil health conditioner: A review, SN Appl. Sci. **2** (2020). doi: https://doi.org/10.1007/s42452-020-3121-5
16. *Sun, Y., Gao, B., Yao, Y., Fang, J., Zhang, M., Zhou, Y., Chen, H., Yang, L.,* Effects of feedstock type, production method, and pyrolysis temperature on biochar and hydrochar properties, Chem. Eng. J. **240** (2014) 574. doi: https://doi.org/10.1016/j.cej.2013.10.081
17. *Kamali, N., Mehrabadi, A. R., Mirabi, M., Zahed, M. A.,* Comparison of micro and nano MgO-functionalized vinasse biochar in phosphate removal: Micro-nano particle development, RSM optimization, and potential fertilizer, J. Water Process. Eng. **39** (2021). doi: https://doi.org/10.1016/j.jwpe.2020.101741
18. *Baronti, S., Vaccari, F., Miglietta, F., Calzolari, C., Lugato, E., Orlandini, S., Pini, R., Zulian, C., Genesio, L.,* Impact of biochar application on plant water relations in *Vitis vinifera* (L.), Eur. J. Agron. **53** (2014) 38. doi: https://doi.org/10.1016/j.eja.2013.11.003

19. *Salehi, S., Habibi, M. J., Anbia, M.,* Synthesis and characterization of amine-modified mesoporous SBA-15 for carbon dioxide sequestration at high pressure and room temperature (RESEARCH NOTE), Int. J. Eng. **29**(10) (2016) 1341.
doi: https://doi.org/10.5829/idosi.ije.2016.29.10a.03
20. *Brassard, P., Godbout, S., Pelletier, F., Raghavan, V., Palacios, J. H.,* Pyrolysis of switchgrass in an auger reactor for biochar production: A greenhouse gas and energy impacts assessment, Biomass Bioenergy **116** (2018) 99.
doi: https://doi.org/10.1016/j.biombioe.2018.06.007
21. *Gao, S., DeLuca, T. H., Cleveland, C. C.,* Biochar additions alter phosphorus and nitrogen availability in agricultural ecosystems: A meta-analysis, Sci. Total. Environ. **654** (2019) 463.
doi: https://doi.org/10.1016/j.scitotenv.2018.11.124
22. *Matuštík, J., Hnátková, T., Kočí, V.,* Life cycle assessment of biochar-to-soil systems: A review, J. Clean. Prod. **259** (2020).
doi: https://doi.org/10.1016/j.jclepro.2020.120998
23. *Zhang, M., Lin, K., Li, X., Wu, L., Yu, J., Cao, S., Zhang, D., Xu, L., Parikh, S. J., Ok, Y. S.,* Removal of phosphate from water by paper mill sludge biochar, Environ. Pollut. **293** (2022) 123.
doi: https://doi.org/10.1016/j.envpol.2021.118521
24. *Dai, L., Wu, B., Tan, F., He, M., Wang, W., Qin, H., Tang, X., Zhu, Q., Pan, K., Hu, Q.,* Engineered hydrochar composites for phosphorus removal/recovery: Lanthanum doped hydrochar prepared by hydrothermal carbonization of lanthanum pretreated rice straw, Bioresour. Technol. **161** (2014) 327.
doi: https://doi.org/10.1016/j.biortech.2014.03.086
25. *Liu, S. B., Tan, X. F., Liu, Y. G., Gu, Y. L., Zeng, G. M., Hu, X. J., Wang, H., Zhou, L., Jiang, L. H., Zhao, B. B.,* Production of biochars from Ca impregnated ramie biomass (*Boehmeria nivea* (L.) Gaud.) and their phosphate removal potential, RSC Adv. **6** (2016) 5871.
doi: https://doi.org/10.1039/C5RA22142K
26. *Rajapaksha, A. U., Chen, S. S., Tsang, D. C. W., Zhang, M., Vithanage, M., Mandal, S., Gao, B., Bolan, N. S., Ok, Y. S.,* Engineered/designer biochar for contaminant removal/immobilization from soil and water: Potential and implication of biochar modification, Chemosphere **148** (2016) 276.
doi: https://doi.org/10.1016/j.chemosphere.2016.01.043
27. *Samaraweera, H., Palansooriya, K. N., Dissanayake, P. D., Khan, A. H., Sillanpää, M., Mlsna, T.,* Sustainable phosphate removal using Mg/Ca-modified biochar hybrids: Current trends and future outlooks, Case Stud. Chem. Environ. Eng. **8** (2023).
doi: https://doi.org/10.1016/j.cscee.2023.100528
28. *Chen, Z., Wu, Y., Huang, Y., Song, L., Chen, H., Zhu, S., Tang, C.,* Enhanced adsorption of phosphate on orange peel-based biochar activated by Ca/Zn composite: Adsorption efficiency and mechanisms, Colloids Surf. A Physicochem. Eng. Asp. **651** (2022).
doi: https://doi.org/10.1016/j.colsurfa.2022.129728
29. *Zhuo, S.-N., Dai, T.-C., Ren, H.-Y., Liu, B.-F.,* Simultaneous adsorption of phosphate and tetracycline by calcium modified corn stover biochar: Performance and mechanism, Bioresour. Technol. **359** (2022).
doi: https://doi.org/10.1016/j.biortech.2022.127477
30. *Zeng, S., Kan, E.,* Sustainable use of $Ca(OH)_2$ modified biochar for phosphorus recovery and tetracycline removal from water, Sci. Total Environ. **839** (2022).
doi: https://doi.org/10.1016/j.scitotenv.2022.156159
31. *Leelatawonchai, P., Laonapakul, T.,* Preparation and characterization of calcium sources from golden apple snail shell for naturally based biomaterials, Adv. Mater. Res. **931–932** (2014) 370.
doi: https://doi.org/10.4028/www.scientific.net/AMR.931-932.370
32. *Wang, Z., Tan, J., Tan, L., Liu, J., Zhong, L.,* Control the egg hatchling process of *Pomacea canaliculata* (Lamarck) by water spraying and submersion, Acta Ecologica Sinica **32**(4) (2012) 184.
doi: https://doi.org/10.1016/j.chnaes.2012.04.008
33. *Horgan, F. G., Stuart, A. M., Kudavidanage, E. P.,* Impact of invasive apple snails on the functioning and services of natural and managed wetlands, Acta Oecol. **54**(1) (2014) 90.
doi: https://doi.org/10.1016/j.actao.2012.10.002
34. *Matsukura, K., Izumi, Y., Yoshida, K., Wada, T.,* Cold tolerance of invasive freshwater snails, *Pomacea canaliculata*, *P. maculata*, and their hybrids helps explain their different distributions, Freshwater Biol. **61**(1) (2016) 80.
doi: https://doi.org/10.1111/fwb.12681
35. *Ketwong, C., Trisupakitti, S., Nausri, C., Senajuk, W.,* Removal of heavy metal from synthetic wastewater using calcined golden apple snail shells, Naresuan. Univ. Sci. Technol. **26**(4) (2018) 61.
36. *Kasmudin, K., Fitria, F., Artiningsih, A.,* The Influence of concentration chitosan of a shell snail to lower levels of BOD and COD on waste laundry, J. Appl. Sci. Eng. Technol. Educ. **4**(1) (2022) 9.
doi: https://doi.org/10.35877/454RI.asci718
37. *Angelova, L., Genova, N., Pencheva, G., Statkova, Y., Yotova, V., Surleva, A.,* Contribution to the molybdenum blue reaction and its application in soil analysis, Methods Objects Chem. Anal. **17**(2) (2022) 59.
doi: https://doi.org/10.17721/moca.2022.59-69
38. *Laonapakul, T., Sutthi, R., Chaikool, P., Mutoh, Y., Chindaprasirt, P.,* Optimum conditions for preparation of bio-calcium from blood cockle and golden apple snail shells and characterization, ScienceAsia **45** (2019) 10.
doi: https://doi.org/10.2306/scienceasia1513-1874.2019.45.010
39. *Laskar, I. B., Rajkumari, K., Gupta, R., Chatterjee, S., Paul, B., Rokhum, S. L.,* Waste snail shell derived heterogeneous catalyst for biodiesel production by the transesterification of soybean oil, RSC Adv. **8** (2018) 20131.
doi: https://doi.org/10.1039/C8RA02397B
40. *Daudzai, Z., Dolphen, R., Thiravetyan, P.,* Simultaneous removal of phosphate and nitrate from synthetic and real wastewater by *Meretrix lusoria* as an efficient and novel material, Water Air Soil Pollut. **232** (2021) 186.
doi: https://doi.org/10.1007/s11270-021-05103-5
41. *Yang, J., Zhang, M., Wang, H., Xue, J., Lv, Q., Pang, G.,* Efficient recovery of phosphate from aqueous solution using biochar derived from co-pyrolysis of sewage sludge with eggshell, J. Environ. Chem. Eng. **9**(5) (2021).
doi: https://doi.org/10.1016/j.jece.2021.105354
42. *Adhikari, S., Gascó, G., Méndez, A., Surapaneni, A., Jegatheesan, V., Shah, K., Paz-Ferreiro, J.,* Influence of pyrolysis parameters on phosphorus fractions of biosolids derived biochar, Sci. Total Environ. **695** (2019).
doi: https://doi.org/10.1016/j.scitotenv.2019.133846
43. *Ramola, S., Belwal, T., Li, C. J., Liu, Y. X., Wang, Y. Y., Yang, S. M., Zhou, C. H.,* Preparation and application of novel rice husk biocharecalcite composites for phosphate removal from aqueous medium, J. Cleaner Prod. **299** (2021).
doi: https://doi.org/10.1016/j.jclepro.2021.126802

44. *Gold, V. F., Bamisaye, A., Adesina, M. O., Adegoke, K. A., Ige, A. R., Adeleke, O., Bamidele, M. O., Alli, Y. A., Oyebamiji, A. K., Ogunlaja, O. O.,* Adsorptive uptake of thymol blue from aqueous medium using calcined snail shells: Equilibrium, kinetic, thermodynamic, neuro-fuzzy and DFT studies, J. Dispersion Sci. Technol. (2024).
doi: https://doi.org/10.1080/01932691.2024.2339458

45. *Adaramaja, A. A., Bamisaye, A., Abati, S. M., Adegoke, K. A., Adesina, M. O., Ige, A. R., Adeleke, O., Idowu, M. A., Oyebamiji, A. K., Bello, O. S.,* Thermally modified nanocrystalline snail shell adsorbent for methylene blue sequestration: Equilibrium, kinetic, thermodynamic, artificial intelligence, and DFT studies, RSC Adv. **14** (2024).
doi: https://doi.org/10.1039/D4RA01074D

46. *Peng, G., Jiang, S., Wang, Y., Zhang, Q., Cao, Y., Sun, Y., Zhang, W., Wang, L.,* Synthesis of Mn/Al double oxygen biochar from dewatered sludge for enhancing phosphate removal, J. Cleaner Prod. **251** (2020).
doi: https://doi.org/10.1016/j.jclepro.2019.119725

47. *Mahato, B. N., Krithiga, T., Thangam, M. M. A.,* Rapid adsorption of As(V) from aqueous solution by ZnO embedded in mesoporous aluminosilicate nanocomposite adsorbent: Parameter optimization, kinetic, and isotherms studies, Surf. Interfaces **23** (2021).
doi: https://doi.org/10.1016/j.surfin.2020.100636

48. *Achelhi, K., Masse, S., Laurent, G., Saoiabi, A., Laghzizil, A., Coradin, T.,* Role of carboxylate chelating agents on the chemical, structural and textural properties of hydroxyapatite, Dalton Trans. **39** (2010) 10644.
doi: https://doi.org/10.1039/C0DT00251H

49. *Sousa de, M. E., Fernández van Raap, M. B., Rivas, P. C., Zelis, P. M., Girardin, P., Pasquevich, G. A., Alessandrini, J. L., Muraca, D., Sanchez, F. H.,* Stability and relaxation mechanisms of citric acid coated magnetite nanoparticles for magnetic hyperthermia, J. Phys. Chem. C. **117** (2013) 5436.
doi: https://doi.org/10.1021/jp311556b

50. *Karimi, M., Hesaraki, S., Alizadeh, M., Kazemzadeh,* A facile and sustainable method based on deep eutectic solvents toward synthesis of amorphous calcium phosphate nanoparticles: The effect of using various solvents and precursors on physical characteristics, J. Non-Cryst. Solids **443** (2016) 59.
doi: https://doi.org/10.1016/j.jnoncrysol.2016.04.026

51. *Dada, A. O., Olalekan, A. P., Olatunya, A. M., Dada, O.,* Langmuir, Freundlich, Temkin and Dubinin–Radushkevich isotherms studies of equilibrium sorption of Zn^{2+} unto phosphoric acid modified rice husk, IOSR J. Appl. Chem. **3**(1) (2012) 38.
doi: https://doi.org/10.9790/5736-0313845

52. *Hoang, L.-T.-T.-T., Phan, H.-V.-T., Nguyen, P.-N., Dang, T.-T., Tran, T.-N., Vo, D.-T., Nguyen, V.-K., Dao, M.-T., Annona glabra* L. seeds: An agricultural waste biosorbent for the eco-friendly removal of Methylene Blue, Arch. Environ. Contam. Toxicol. **86**(1) (2023) 48.
doi: https://doi.org/10.1007/s00244-023-01044-8

53. *Hoang, L.-T.-T.-T., Phan, H.-V.-T., Nguyen, N.-N., Dang, T.-T., Tran, T.-N., Nguyen, V.-K., Dao, M.-T.,* Utilization of dragon fruit (*Hylocereus undatus*) peel-derived biochar for the adsorptive removal of tetracycline from aqueous solution, Int. J. Phytorem. **14**(26) (2024) 2313.
doi: https://doi.org/10.1080/15226514.2024.2389471

54. *Yao, Y., Gao, B., Chen, J., Yang, L.,* Engineered biochar reclaiming phosphate from aqueous solutions: Mechanisms and potential application as a slow-release fertilizer, Environ. Sci. Technol. **47** (2013) 8700.
doi: https://doi.org/10.1021/es4012977

55. *Lu, S. G., Bai, S. Q., Zhu, L., Shan, H. D.,* Removal mechanism of phosphate from aqueous solution by fly ash, J. Hazard. Mater. **161** (2009) 95.
doi: https://doi.org/10.1016/j.jhazmat.2008.02.123

56. *Liu, X., Yang, S., Liu, S., Yang, Y.,* Performance and mechanism of phosphorus removal by slag ceramsite filler, Process Saf. Environ. Prot. **148** (2021) 858.
doi: https://doi.org/10.1016/j.psep.2021.02.016